
TOWARDS EXPLAINABLE CONVERSATIONAL AI FOR EARLY DIAGNOSIS WITH LARGE LANGUAGE MODELS

Maliha Tabassum

Department of Information and Communication Technology
 Bangladesh University of Professionals
 Dhaka 1216, Bangladesh
 maliha2154901035@student.bup.edu.bd

Dr. M. Shamim Kaiser

Institute of Information Technology
 Jahangirnagar University
 Dhaka 1342, Bangladesh
 mskaiser@juniv.edu

December 22, 2025

ABSTRACT

Healthcare systems around the world are grappling with issues like inefficient diagnostics, rising costs, and limited access to specialists. These problems often lead to delays in treatment and poor health outcomes. Most current AI and deep learning diagnostic systems are not very interactive or transparent, making them less effective in real-world, patient-centered environments. This research introduces a diagnostic chatbot powered by a Large Language Model (LLM), using GPT-4o, Retrieval-Augmented Generation, and explainable AI techniques. The chatbot engages patients in a dynamic conversation, helping to extract and normalize symptoms while prioritizing potential diagnoses through similarity matching and adaptive questioning. With Chain-of-Thought prompting, the system also offers more transparent reasoning behind its diagnoses. When tested against traditional machine learning models like Naive Bayes, Logistic Regression, SVM, Random Forest, and KNN, the LLM-based system delivered impressive results, achieving an accuracy of 90% and Top-3 accuracy of 100%. These findings offer a promising outlook for more transparent, interactive, and clinically relevant AI in healthcare.

Keywords :

LLM, Explainable AI, Retrieval-Augmented Generation, Top-3 Accuracy, Conversational Diagnostics

1 Introduction

One of the most significant issues in the world is healthcare. The issues such as poor diagnosis systems, extremely expensive healthcare services, and lack of physicians and experts are common in many countries. The problems can cause delays in the treatment process and result in ill health. In Bangladesh, things are also not encouraging. As an example, in 2022, people spent roughly 61 USD per capita on healthcare², yet health spending was only 2.39 percent of GDP¹. Almost 44 USD per capita of this was directly out of the own cash of people³. This implies that majority of families are forced to pay their treatment with their own money and this is very hard to many individuals.

The lack of affordable and accessible healthcare demonstrates the necessity of intelligent solutions. The traditional AI and machine learning models have proven to be promising in the healthcare domain, yet they have certain significant issues. The majority of these models are very inflexible that they only match the precise symptoms to diseases. This causes difficulty in communicating with the patients effectively as real people tend to define their health using different words. To top that, such models tend to be somewhat like a black box, that is, it is hard to trace the way certain symptoms cause the ultimate forecast. Such a lack of transparency decreases the level of trust and renders the systems less patient-centric services.

²<https://data.worldbank.org/indicator/SH.XPD.CHEX.PC.CD?locations=BD>

¹<https://data.worldbank.org/indicator/SH.XPD.CHEX.GD.ZS?locations=BD>

³<https://data.worldbank.org/indicator/SH.XPD.OOPC.PC.CD?locations=BD>

However, the Large Language Models (LLMs) are different. They are able to have natural conversations like a patient conversing with a clinician. Rather than relying on precise vocabulary or the use of specific patterns, LLMs are able to interpret the meaning of a description given by a patient of symptoms. This is flexible, as it enables them to offer a more interactive, transparent and human support in the diagnosis process.

Even with these developments, there have been vast gaps in the existing research in the methods of diagnosis. To begin with, high-performance models cannot be explained: Deep learning models are highly accurate, but they are typically black boxes that do not explain why they behave in a certain way. Their application in diagnostic conversations has not been thoroughly studied even with the XAI integration. Second is a lack of attention to conversational diagnostic situations: The bulk of the research is devoted to structured data processing as opposed to the dynamic and iterative aspects of clinician-patient interaction. This is starting to be addressed by studies based on LLM and requires expansion. Third, dynamic knowledge integration is lacking: A lot of systems are based on fixed datasets, and cannot automatically refresh with fresh medical knowledge, which restricts their flexibility to changing diseases or changes in symptoms. Lastly, there is the absence of adaptive questioning depending on the context of the disease: The existing diagnostic systems have fixed sets of questions, which do not dynamically respond to the actual diagnosis context.

Both communicable and non-communicable diseases have a huge burden globally. In 2021, the number of cases and deaths caused by malaria was estimated to be 263 million cases and 597000 deaths globally with 95 percent of the fatalities reported in Africa World Health Organization [2024c]. Mycobacterium tuberculosis causes Tuberculosis (TB), which in 2023 had afflicted almost 10.8 million people and caused nearly 1.25 million deaths World Health Organization [2024d]. By April 2024, dengue fever, an infectious disease spread by mosquitos, had reached a record high of more than 7.6 million cases (3.4 million confirmed), and more than 3 000 deaths, already surpassing the 2023 figures World Health Organization [2024b]. Chronic hepatitis B infection is still prevalent, and it is estimated that there are approximately 254 million individuals with the virus in 2022 and that over 1.1 million deaths are linked to the infection each year elsewhere World Health Organization [2023a]. Asthma was one of the respiratory diseases with an incidence of approximately 262 million individuals and a death burden of approximately 455000 in 2019 World Health Organization [2019b]. Digestive diseases are also common: gastro-esophageal reflux disease (GERD) had an estimated global prevalence of approximately 825.6 million cases in 2021 GBD 2021 Gastrointestinal Disorders Collaborators [2022] and irritable bowel syndrome (IBS) has a pooled world-wide prevalence of about 14.1 % Ford, Sperber, and et al. [2020]. The most prevalent nutritional disorder is iron-deficiency anemia, which is experienced by approximately 1.92 billion individuals (approximately 24.3 percent of the global population) in 2021 GBD 2021 Anaemia Collaborators [2023]. Acute diarrhoeal disease resulted in approximately 1.7 billion childhood episodes per year and 444000 deaths in children under five years of age per year World Health Organization [2020]. Mental disorders are equally very heavy burdens: depression impacts almost 280 million individuals World Health Organization [2019c] and anxiety disorders impact nearly 301 million World Health Organization [2019a]. Seasonal viral fevers like influenza cause a burden of about 1 billion cases per year, 3-5 million severe cases, and 290-650 thousand deaths, with over 775 million confirmed cases and 7 million deaths as of mid-2024 being due to COVID-19 World Health Organization [2024a] compared to 775 million cases and 7 million deaths per year. Lastly, neurological diseases including migraine were present in approximately 1.16 billion individuals in 2021, up 58 percent since 1990 GBD 2021 Headache Collaborators [2023]. All of these numbers highlight the ongoing and pervasive nature of global health issues.

The significant contributions of this research are:

- Complex conversational diagnostic scenarios of the LLM-based system was compared to traditional ML models to evaluate the improvements in performance.
- Explainable AI mechanisms were incorporated to provide more insight into the diagnostic process and make it interpretable to make informed decisions.
- A user-friendly, conversational, and diagnostic system with one of the LLMs that could identify diseases with precision was developed.
- The efficacy of the whole system in promoting the quality and accessibility of diagnosis in a healthcare setting was measured.
- In order to achieve a higher diagnostic accuracy and user engagement, real-time symptom tracking and adaptive generation of questions were introduced.

This research begins with Section 2, which reviews existing studies on artificial intelligence diagnostic methods and the datasets used in healthcare. Section 3 introduces the background technologies and tools, methodology and system architecture. Section 4 presents the results, focusing on system performance, explainability, and comparisons with traditional machine learning approaches. Finally, Section 5 concludes with the key findings and outlines possible future research directions.

2 Related Work

2.1 Recent ML/DL Approaches

In the last 10 years, machine learning (ML) and deep learning (DL) have remarkably reshaped medical diagnostics, even to a point of approaching expert-level performance in tasks such as detecting retinal diseases, interpreting pathology and radiology, and so on. The initial research has shown the possibilities of medical use of a high stakes of DL. As an example, a 3D convolutional neural network (CNN) of optical coherence tomography (OCT) scan was created by De Fauw, Ledsam, Romera-Paredes, and et al. [2018], which demonstrated referral ratings on a par with experts in detecting retinal diseases. In a similar fashion, Esteva, Kuprel, Novoa, and et al. [2017] used CNNs in the skin cancer classification task on the ISIC dataset 2016 and achieved 72.1% of dermatologist-level accuracy, whereas Gulshan, Peng, Coram, and et al. [2016] trained a DL model on retinal fundus images and obtained high sensitivity and specificity in diabetic retinopathy detection. In cardiology, Poplin, Varadarajan, Blumer, and et al. [2018] showed that retinal images had forecasting abilities of cardiovascular risk factors with an AUC of 0.97 age and 0.71 smoking status.

DL has as well developed pathology and radiology. As demonstrated by Ehteshami Bejnordi, Veta, Johannes van Diest, and et al. [2017], the weakly supervised DL was able to identify the lymph node metastases in breast cancer with AUC of more than 0.98 and active on 44,732 whole-slide images of prostate, breast, and basal cell carcinoma with AUC of over 0.98, as shown by . Campanella, Hanna, Geneslaw, and et al. [2019]. Rajpurkar, Irvin, Zhu, and et al. [2018] introduced CheXNet in the chest radiography which is more successful than the earlier automated systems with an AUC of 0.862 at detecting atelectasis. Abràmoff, Lavin, Birch, and et al. [2018] also indicated the clinical usefulness of AI using an autonomous diabetic retinopathy system in primary care clinics with the highest sensitivity of 97.6% to evaluate immediately. All these foundational works underscore the high accuracy of the DL/ML models in different imaging modalities, but most of them are only single-turn and modality-specific in their analysis and offer limited clinical decision-making interpretability Topol [2019].

In addition to the recent researches have expanded the capabilities of ML/DL to multi-modal and complex clinical settings. In 2024, Omar, Smith, and et al. [2024] conducted a systematic review and screened deep learning applications in spondyloarthropathy (SpA) imaging (MRI, CT, and X-ray) and found that advanced CNNs and U-Net architectures reported AUCs reaching 0.98 on a par with expert radiologists. Vazquez, Liu, and et al. [2025] conducted a review of 153 articles on the application of machine learning and deep learning to cervical cancer, and they found that AI is increasingly used in the diagnosis, prediction, and prognosis of cervical cancer. In addition, Song, Kim, and et al. [2025] established a DL-assisted method of diagnosing acute mesenteric ischemia based on CT angiography in combination with clinical information that had high diagnostic accuracy and the possibility of early diagnosis in the emergency room.

Whereas early DL/ML models were excellent in single-modality tasks, these new publications show the pattern of client-focused, clinically combined AI models, capable of processing multiple data types, enhancing understandability, and decision-making. However, the issues with the seamless inclusion of these models into clinical processes and the high degree of interpretability still persist, which is why AI-based medical diagnosis still remains an open problem.

2.2 LLM-Based Approaches

Tu, Palepu, Schaeckermann, Saab, Freyberg, Tanno, Wang, Li, Amin, Tomasev, Mahdavi, Semturs, Gottweis, Barral, Chou, Corrado, Matias, Karthikesalingam, and Natarajan [2024] proposed AMIE, a multi-turn medical dialogue conversational diagnostic large language model (LLM). Their system was accurate when identifying rare diseases with high diagnostic accuracy (89.4%). Nevertheless, AMIE was not interpretable at a fine-grained level, which restricted the understanding of how single symptoms affected the diagnostic results, which is essential in clinician trust and decision-making. Singhal, Azizi, Tu, Mahdavi, Wei, Chung, Scales, Tanwani, Cole-Lewis, Pfohl, Payne, Seneviratne, Gamble, Kelly, Scharli, Chowdhery, Mansfield, y Arcas, Webster, Corrado, Matias, Chou, Gottweis, Tomasev, Liu, Rajkomar, Barral, Semturs, Karthikesalingam, and Natarajan [2022] developed Med-PaLM, a medical adaptation of Google PaLM based on clinical datasets including MedQA and PubMedQA and fine-tuned on them. Their work made a huge progress in the field of medical question answering delivering 67.6% accuracy and better than the preceding models. Nevertheless, Med-PaLM's interaction was still non-conversational and unbending, which could not dynamically respond to user inputs and offer understandable reasoning, which is a major limitation to the use of the method in the real world in diagnosis.

Gupta, Singh, Manikandan, and Ehtesham [2025] compared GPT-4 and other LLMs in symptom-based disease diagnosis with a 91.3% accuracy. Although this research confirmed the diagnostic opportunities of foundation models, it was based on fixed prompts and failed to provide interactive dialogue and monitoring of the symptoms, which limits its use in real-life clinical practice. Kim et al. [2024] proposed MDAgents, a system in which a set of LLMs work

Table 1: Summary of Key ML/DL Diagnostic Studies

Reference	Methodology	Dataset / Domain	Accuracy / Performance
De Fauw et al. [2018]	3D OCT scan analysis using deep CNN	14,884 retinal scans	Expert-level referral recommendations
Esteva et al. [2017]	CNN for skin cancer classification	ISIC 2016 dataset	72.1% overall accuracy
Gulshan et al. [2016]	Deep learning for diabetic retinopathy detection	Retinal fundus photographs	High sensitivity & specificity
Poplin et al. [2018]	Deep learning for cardiovascular risk prediction	284,335 retinal images	AUC: age = 0.97, smoking = 0.71
Ehteshami Bejnordi et al. [2017]	DL for lymph node metastasis detection	CAMELYON16 dataset	AUC > 0.98
Campanella et al. [2019]	Weakly supervised DL for pathology images	44,732 whole-slide images	AUC > 0.98 (prostate, breast, basal cell carcinoma)
Rajpurkar et al. [2018]	Deep learning for chest radiographs (CheXNet)	ChestX-ray14 dataset	AUC for atelectasis = 0.862
Abràmoff et al. [2018]	Autonomous AI for diabetic retinopathy	Primary care clinics	Sensitivity = 97.6%
Omar et al. [2024]	Review of DL for spondyloarthropathy imaging	MRI, CT, X-ray	AUC \approx 0.98 (expert-level)
Vazquez et al. [2025]	Review of ML/DL in cervical cancer	153 articles reviewed	AI widely used for diagnosis, prediction, prognosis
Song et al. [2025]	DL-assisted diagnosis of acute mesenteric ischemia	CT angiography + clinical data	High diagnostic accuracy (early ER detection)

together to complete a complex diagnostic problem. This method proved to be promising in the process of coordinating various models of differential diagnosis. Nonetheless, it has been only assessed in terms of benchmarks and artificial activities, and the actual interactions with patients and explainability remain under-investigated. Toma, Lawler, Ba, et al. [2023] applied a dialogue-based LLM to encode clinical knowledge to predict diseases. Whereas the model had high benchmark performance, it was not tested in full clinician dialogues and had not been tested exhaustively in regard to transparent reasoning or real-world robustness.

All of these studies demonstrate the rapid development of LLMs in healthcare, though also suggest that the gaps in this field are still quite considerable and in particular, explainability, conversational adaptability, and real-time symptom monitoring still have not been fully addressed.

3 System Architecture and Methodology

3.1 Background Tools & Technologies

The diagnostic platform is developed on the basis of the advanced libraries and frameworks that are oriented to process medical data, language translation, and machine learning. The system is based on these technologies that provide stability, efficiency, and precision of the diagnostic process.

3.1.1 RAG Architecture

Our system uses the Retrieval Augmentation Generation (RAG) structure, which incorporates the advantages of retrieval-based and generative AI systems. FAISS is applied to find the pertinent medical knowledge effectively, and the models of Azure OpenAI give helpful, context-aware answers. The RAG architecture takes the medical records, stitches in patient queries and applies AI to come up with the correct diagnostic output depending on the context retrieved. This is a RAG system workflow of a simple system. 1.

Table 2: LLM-Based Diagnostic Methods

Reference	Methodology	Dataset / Domain	Accuracy / Performance
Tu et al. [2024]	AMIE: Multi-turn conversational LLM	302 rare disease cases	89.4%
Singhal et al. [2022]	Med-PaLM: Fine-tuned medical LLM	MedQA, PubMedQA, clinical records	MedQA: 67.6%, MedMCQA: 57.6%, PubMedQA: 79.0%
Gupta et al. [2025]	GPT-4 and other LLMs for symptom-based diagnosis	Multiple clinical and organizational records	91.3%
Kim et al. [2024]	MDAgents: Multi-agent LLM collaboration for differential diagnosis	Benchmark diagnostic datasets	average accuracy improvement of 11.8%
Toma et al. [2023]	Clinical Camel: Dialogue-based LLM encoding clinical knowledge	Clinical case studies	USMLE: 64.3%, PubMedQA: 77.9%, MedQA: 60.7%, MedMCQA: 54.2%

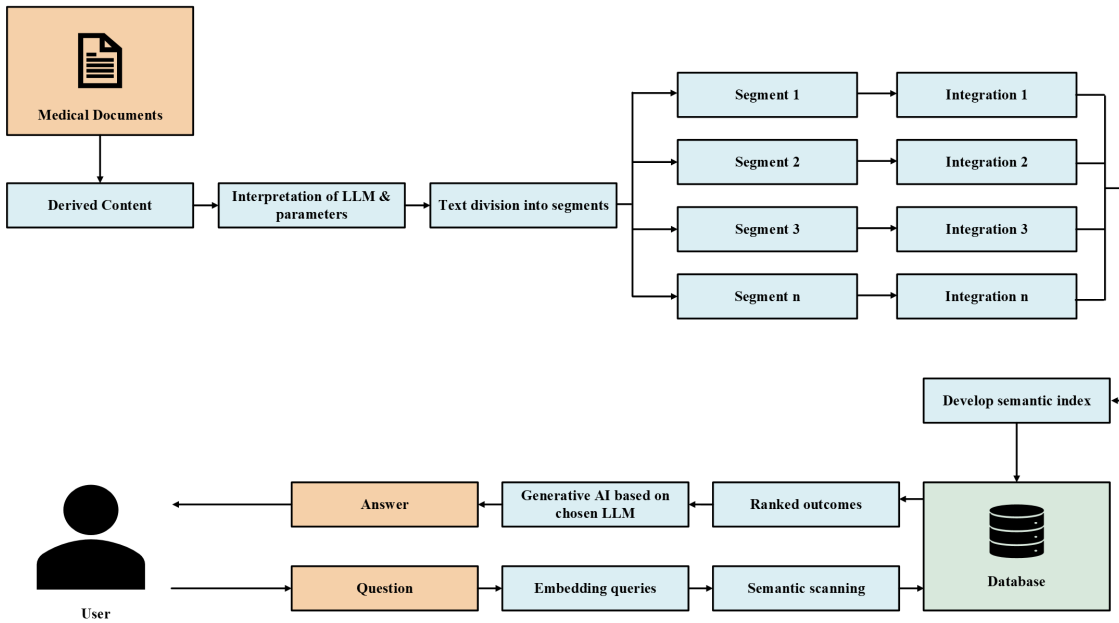


Figure 1: Workflow of a Simple RAG based System

3.1.2 Azure OpenAI Services and LangChain Framework

AzureChatOpenAI: This serves as the main interface, providing access to OpenAI's GPT-4o model through Azure's cloud infrastructure. The system ensures consistency with a temperature setting of 0.3 and keeps the output concise with a token limit of 50. Retry mechanisms are built in to handle potential API failures, ensuring system reliability in medical applications Microsoft Azure [2023b].

AzureOpenAIEMBEDDINGS: This application is used to transform medical texts into numerical vectors, which allows matching patient inquiries with the applicable medical knowledge with high precision. It assists the system to comprehend the environment of patient symptoms and match them with medical jargon Microsoft Azure [2023a].

LangChain Framework:

- **LLMChain:** The core orchestration module, combining patient input with medical knowledge to generate accurate disease predictions and maintain consistent diagnostic protocols Chase [2023].
- **PromptTemplate:** Helps structure the language model's output by ensuring that responses are limited to disease names, avoiding unnecessary explanations and maintaining clarity in the diagnostic process LangChain [2023a].
- **RecursiveCharacterTextSplitter:** This tool segments lengthy medical documents into manageable chunks, maintaining context and allowing effective information retrieval LangChain [2023b].

3.1.3 Document and Data Processing

FAISS (Facebook AI Similarity Search): This vector storage and retrieval tool allows for efficient matching of patient queries with relevant medical knowledge, ensuring fast and accurate responses from the system, even with large datasets Facebook AI [2023].

PyPDF2: This library aids in extracting text from PDFs with complex layouts, enhancing the document processing pipeline and supporting various medical document formats Phaseit [2023].

Scikit-learn Metrics: We used Scikit-learn's metrics module to evaluate system performance. It helps measure accuracy, precision, recall, and F1-score, providing valuable insights for continuous improvement of the diagnostic model Scikit-learn [2023].

Pandas and NumPy: Pandas manages the data pipeline, tracking patient data, diagnostic results, and metrics Pandas [2023]. NumPy facilitates efficient numerical computations, especially for operations involving similarity searches and embeddings NumPy [2023].

Matplotlib: This library was used to visualize the system's performance, allowing us to compare the effectiveness of LLM-based diagnostics with traditional machine learning models Matplotlib [2023].

3.2 System Overview

Our diagnostics system is made of two stages. The first stage is symptom based diagnosis in which the system requests the user to provide information on some of the symptoms and interprets the data provided to create top 3 probable diseases. Once the necessary conditions of substantial information was reached, the second step was to proceed to the next step where the system inquires on certain test reports of lab tests concerning the related disease and eventually give the probable diseases according to the user response. Figure 2 illustrates the overall architecture.

1. **User Input & Symptom Parsing:** The system starts by taking the input of the user in terms of their symptoms. It then works on this information to enable it know more about the symptoms.
2. **Generate Candidate Diseases:** Depending on the input symptoms, the system would provide a list of potential diseases that may also be the cause of the input symptoms.
3. **Phase 1: Symptom Ilicitation:** The system proceeds to give follow up questions to gather more information. This is aimed at reducing the list of potential diseases. A system that has not posed sufficient questions and has fewer than 8 symptoms will prompt more questions to obtain more information.
4. **Phase 2: Test-Based Diagnosis:** When the system thinks it is prepared to arrive at a more precise diagnosis, it goes to Phase 2. In this case, it implies medical examinations according to the symptoms and the available amount of knowledge about the condition.
5. **Display Supporting Information:** Once the relevant data has been gathered, the system expresses the corresponding information, i.e. symptoms, test findings, and risk factors that justify the diagnosis.

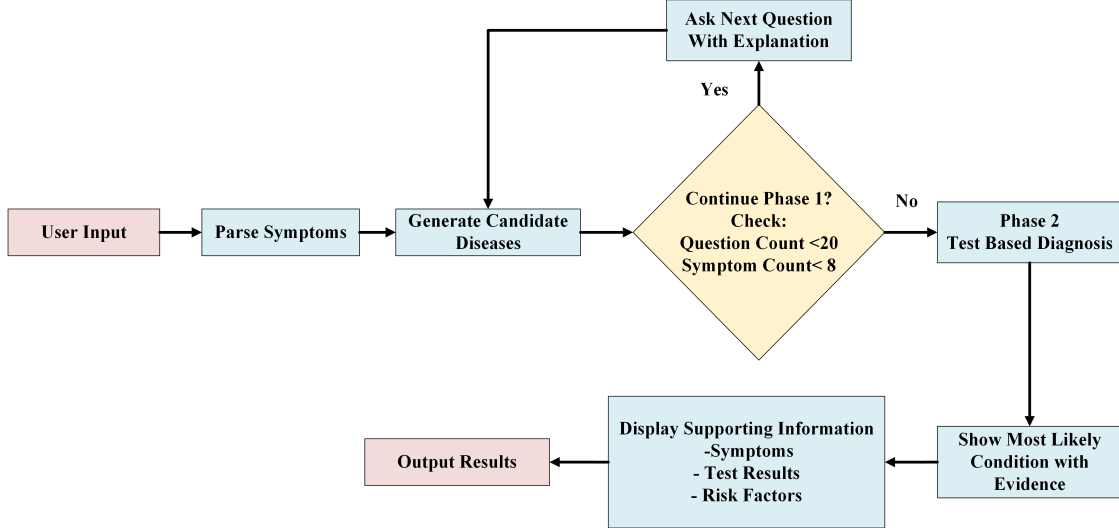


Figure 2: System Architecture

6. **Show Most Likely Condition with Evidence:** Finally, the system presents the most likely condition, supported by the evidence collected from the conversation and any tests recommended. This helps the user understand the reasoning behind the diagnosis.

In simpler terms, this system functions like an interactive assistant that asks questions, suggests tests, and helps identify the most likely health issue based on user responses.

Figure 2 shows the workflow of the RAG system, which forms the foundation of our knowledge retrieval mechanism.

3.3 Knowledge Base Construction

We constructed a comprehensive medical knowledge base covering 14 diseases such as- Malaria, Tuberculosis, Dengue Fever, Hepatitis B, Asthma, Gastroesophageal Reflux Disease (GERD), Irritable Bowel Syndrome (IBS), Iron-Deficiency Anemia, Acute Diarrheal Illness, Depression, Anxiety Disorders, Viral Fever, Covid-19 and Migraine. across four categories. Table 3 shows the distribution of diseases in our knowledge base.

Table 3: Disease Categories in Medical Knowledge Base

Disease Category	Number of Diseases
Infectious Diseases	6
Chronic Conditions	4
Mental Health	2
Other Common Conditions	2
Total	14

The knowledge base was constructed by scraping information from authoritative publicly accessible sources, including guidelines and reports published by the World Health Organization (WHO) and other established medical organizationsWorld Health Organization [2024g,i,h, 2023c, 2024j,b], Centers for Disease Control and Prevention [2024a], World Health Organization [2023a, 2015, 2019b], National Center for Biotechnology Information [2023a], World Gastroenterology Organisation [2021], Rome Foundation [2016], National Center for Biotechnology Information [2023b], World Health Organization [2024e, 2020, 2019c, 2023b, 2019a], Centers for Disease Control and Prevention [2024b], Mayo Clinic [2024], World Health Organization [2024f], International Headache Society [2018a,b] . Here is a flow chart of data collection process in Figure 3

One of the most effective ways to obtain the similarity between vectors is - Jaccard Similarity. As the disease information are stored in the database as vectors, it can be substantial to compare the similitude of symptoms across the listed diseases. Symptom similarity analysis using Jaccard similarity coefficients revealed significant overlap between certain conditions. Figure 4 shows a heatmap of symptom similarity across diseases, with Viral Fever and COVID-19 showing

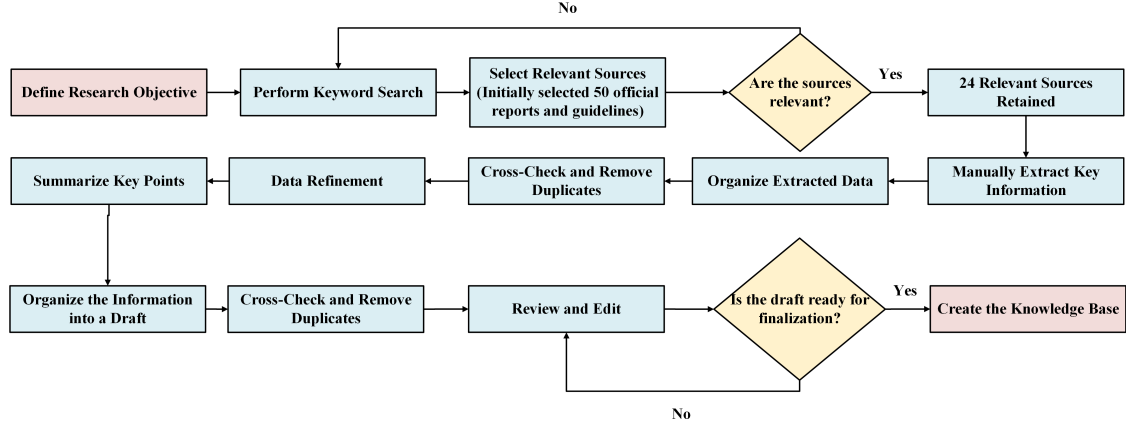


Figure 3: Workflow of Knowledge Base Construction

0.53 similarity, indicating nearly half their symptoms overlap- which is expected as their manifestations can be quite similar. In addition to that, no other set of diseases show a significant amount of likelihood, which can be an indication that the symptoms listed for each diseases were more or less unique which can serve as a strong factor for accurate diagnosis.

The knowledge base contains four types of information for each disease:

1. **Symptoms:** Standardized descriptions of clinical manifestations, weighted by severity and diagnostic significance.
2. **Risk Factors:** Demographic, environmental, and lifestyle factors associated with increased disease risk.
3. **Threshold Values:** Quantitative diagnostic criteria from laboratory tests and clinical measurements.
4. **Management Information:** Evidence-based treatment recommendations and referral guidelines.

3.3.1 Data Preprocessing

After collecting the data from PDFs and online sources, it goes through a cleaning and organizing process to make it ready for the chatbot.

The content is split into primary sections which are symptoms, risk factors, and diagnostic criteria, with the help of regular expressions. This renders the data of each and every disease well organized. Afterward, the symptoms are given different levels of importance according to severity. The greater the severity of the symptoms, i.e., the chest pain or fatigue, the stronger the impact that a symptom will produce and the more precise will be the chatbot priority in case of conditions that are more critical.

After a thorough cleaning and structuring of the data, it is saved in a Pandas DataFrame. Such arrangement allows searches and retrieval of pertinent information with ease particularly when combined with Retrieval-Augmented Generation (RAG) system that assists the chatbot in locating the appropriate information in dialogue.

3.3.2 Integration into the System

The RAG system is linked with the knowledge base, which enables the chatbot to mention significant data in the course of chatting with users. The system absorbs a pre-trained language model along with a knowledge retrieval system making it accurate in diagnosis.

In order to conduct semantic searches, the disease-related information is converted into vectors with the help of FAISS. This serves the purpose of the chatbot to make it easy to find the most recent information in correspondence to the queries of the user. The information is also transformed into the Sentence-Transformer embedding representing implicit meanings of the symptoms, the risk factors, and diagnostic criteria. This enhances the skill of the chatbot in aligning the question of the users with the knowledge base.

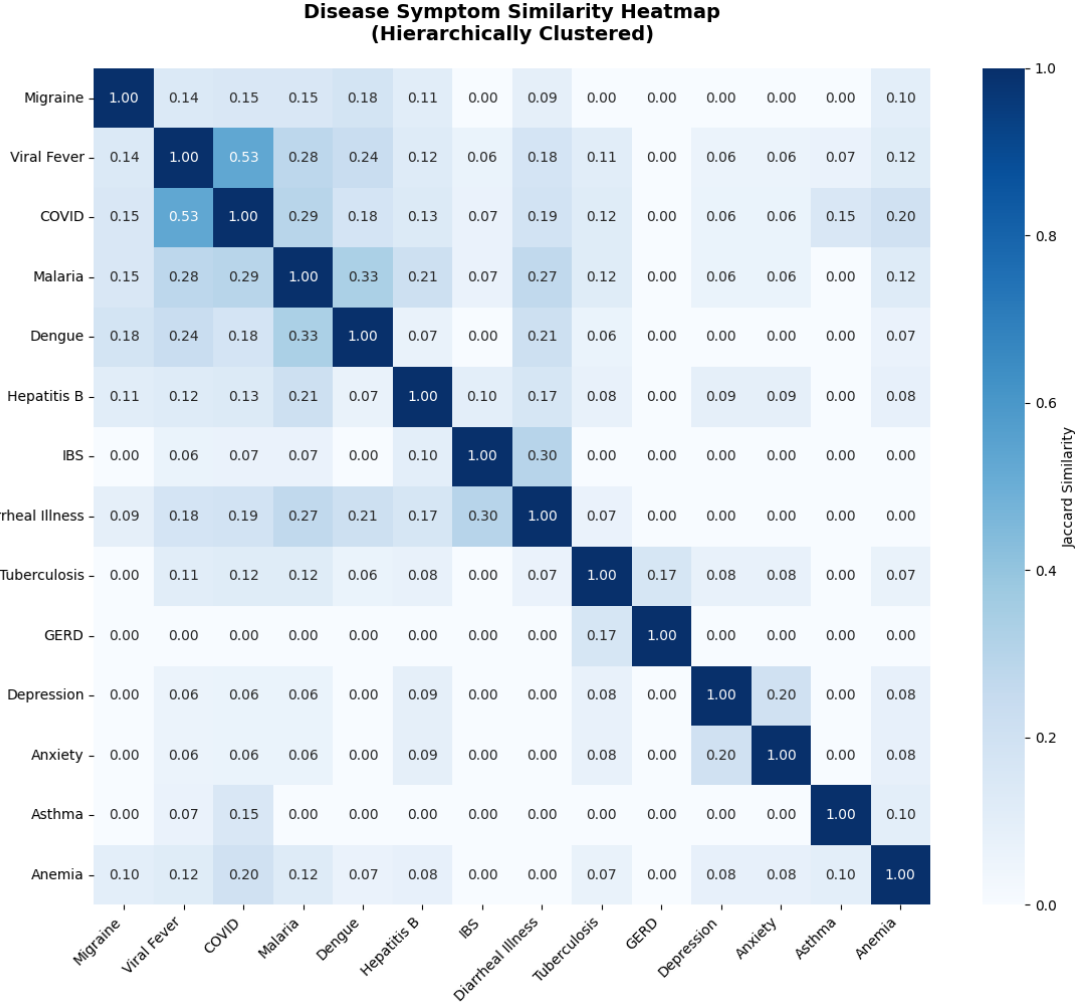


Figure 4: Disease Symptom Similarity Heatmap using Jaccard Similarity Coefficients

3.4 Preprocessing of Input Data

The preprocessing of the user input is an important stage of data analysis preparation. The step will make the raw data to be arranged and in a format that will be utilized by the chatbot. It is then tokenized into smaller units (such as words or phrases) to make it easier to analyze the text. For instance, the sentence "I have a headache and a fever" becomes ["I", "have", "a", "headache", "and", "a", "fever"].

Next, common words like "the", "and", and "is" (called stopwords) are removed because they don't contribute much meaning. This reduces unnecessary data and makes the analysis more efficient. Finally, normalization is done by converting all text to lowercase and removing irrelevant characters, like punctuation, ensuring everything is consistent and easier to work with.

3.5 Document Processing and Retrieval System

The RAG system handles medical documentation in a number of processes. PyPDFLoader is used to extract text in medical PDFs. The documents are then divided into blocks of 1000 characters with 200-character overlap in order to make the processing easier. Afterward, the system creates the text in the form of vectors with the help of sentence-transformers. These embeddings are compiled in FAISS, and can be quickly accessed when interacting with the user.

The retrieval system is based on converting user queries into embeddings with the same model as document chunks. The best-k most relevant chunks of documents then are searched by similarity. The context retrieved assists the LLM to produce the right response.

3.6 Conversation Management System

3.6.1 Symptom Tracker

The symptom tracker serves as the memory of the consultation, which retains both confirmed and rejected symptoms reported by the patient as well as the record of questions that have been posed. Denied symptoms decrease the probability of diseases, computed by means of the formula:

$$\tau_s = -0.8 \times w_s \quad (1)$$

where w_s is the original diagnostic weight of the symptom. The disease score is updated dynamically as:

$$\text{Score}(d) = \sum_{\text{matched } s} \alpha_s \cdot w_s - \sum_{\text{denied } s} \tau_s \quad (2)$$

where $\alpha_s = 1.0$ for exact matches and $\alpha_s = 0.6$ for semantic matches.

3.6.2 Dynamic Question Generation

The selection of questions is guided by the ability to distinguish between diseases. The system first ranks diseases by their current confidence scores and identifies the symptoms associated with the top diseases that haven't yet been asked about. If no symptoms are left to ask, the system expands the list to include symptoms from the full knowledge base. The most informative symptom is then selected and justified, ensuring that each question either confirms or rules out high-likelihood diseases, bringing the system closer to a confident diagnosis.

3.7 Diagnostic Engine

3.7.1 Symptom Matching Phase

The first step in the diagnostic engine is to match patient-reported symptoms with the knowledge base. Exact or synonym matches contribute their full weight to the disease scores, while semantic matches—determined by cosine similarity between embeddings—contribute 60%. The similarity is computed as:

$$\text{sim}(u, s) = \frac{E(u) \cdot E(s)}{\|E(u)\| \cdot \|E(s)\|} \quad (3)$$

where $E(\cdot)$ represents the embedding function for a symptom or user-reported expression.

3.7.2 Per-Disease Confidence Estimation

The confidence of each disease hypothesis C_d is computed through a nonlinear combination of base score, number of matched symptoms, and penalties for denied symptoms:

$$\text{base_confidence} = 1 - e^{-0.15S_d} \quad (4)$$

$$\text{symptom_factor} = \min\left(\frac{\ln(1 + n_d)}{4.0}, 0.5\right) \quad (5)$$

$$\text{negative_factor} = \min(0.15N_d, 0.6) \quad (6)$$

$$\text{raw_conf} = \text{base_confidence} + \text{symptom_factor} - \text{negative_factor} \quad (7)$$

$$C_d = \max(0, \min(0.9 \times \text{raw_conf}, 0.95)) \quad (8)$$

where S_d is the disease's accumulated base score, n_d is the number of matched symptoms, and N_d is the cumulative penalty from denied symptoms. This formulation caps confidence below 1.0 and enforces smooth growth with diminishing returns.

3.7.3 Overall Diagnostic Confidence

The final diagnostic confidence C_{overall} is computed using the top disease's score and its margin over the second-highest score:

$$\text{margin} = \begin{cases} \frac{S_{\text{top}} - S_2}{S_{\text{top}}}, & S_2 > 0 \\ 1.0, & \text{otherwise} \end{cases} \quad (9)$$

$$\text{raw} = (n_{\text{top}} \times 0.10) + (\text{margin} \times 0.25) + (S_{\text{top}} \times 0.12) - \min(0.05N_{\text{top}}, 0.5) \quad (10)$$

$$C_{\text{overall}} = \tanh(\text{raw}) \times 0.9 \quad (11)$$

where n_{top} and N_{top} denote the number of matched symptoms and denied symptoms penalty for the top-ranked disease respectively.

Logarithmic and exponential transformations were also purposely used to avoid overconfidence, and to come up with more calibrated diagnostic probabilities. The logarithmic form of expression, which is of the nature of $\ln(1 + n_d)$, makes sure to maintain diminishing returns; this is that with the increasing number of symptoms matched, the confidence increases less and less, avoiding inflation of confidence in case the number of overlapping or non-specific symptoms matched is large. The base score is stabilized by the exponential term, $1 - e^{-0.15S_d}$, which causes the function to saturate with increasing evidence. Lastly, the hyperbolic tangent is used (as the hyperbolic tanh) to make the total confidence bounded, so that it can scale smoothly and confidence extreme changes are avoided. A combination of these nonlinearities reduces bias and overconfidence, providing conservative but high-quality diagnostic confidence estimates.

3.8 LLM Integration

3.8.1 Prompt Templates

The large language model (LLM) uses specialized prompts to ensure reliable performance across the medical domain. These prompts include:

1. **Symptom Extraction:** Extracts relevant symptoms from patient text using retrieval context.
2. **Follow-up Symptom Extraction:** Identifies new symptoms in patient responses to targeted questions.
3. **Normalization:** Standardizes raw symptom phrases into medical terms.
4. **Dynamic Question Generation:** Selects the next most informative symptom to ask about.
5. **Test Question Generation:** Formulates patient-friendly questions about diagnostic tests.
6. **Test Result Interpretation:** Interprets test results against stored thresholds.
7. **Risk Factor Evaluation:** Asks about unaddressed risk factors for specific diseases.
8. **Final Diagnosis Synthesis:** Combines symptoms, hypotheses, test results, and exclusions into a logical conclusion.

3.8.2 Chain Orchestration

It starts with an open-ended elicitation process and then goes over to targeted iterative questioning. The questioning is to be continued until the condition of confirming at least 8 symptoms are fulfilled. Though this cutoff might seem high, the procedure is still feasible since the system has a built-in database of medically relevant terms and synonymous phrases of each symptom and can thus perform a more efficient match and recognition even when patients might be using different and informal language.

In case these requirements have been met or the limit of 20 questions have been achieved, the system proceeds into the test evaluation stage. The last step is a synthesis prompt that integrates the symptoms, test results, and risk factors into a unified diagnosis report to balance the extent of diagnostic completeness and diagnostic accuracy.

3.9 Introducing Explainability

3.9.1 Justification for Symptom Question Selection

In cases of dynamic questioning, every follow-up symptom is thoroughly selected according to clinical logic 5. The system involves the application of active diagnostic hypotheses and the attention to the least-asked symptoms that may distinguish the diseases. The symptoms are prioritized as long as they are relatively confirmed or disproved and the degree to which confidence of the best disease candidates is seriously influenced. This methodology maintains a narrow and effective questioning process and the rationale underlying any question is easily understandable and clear.

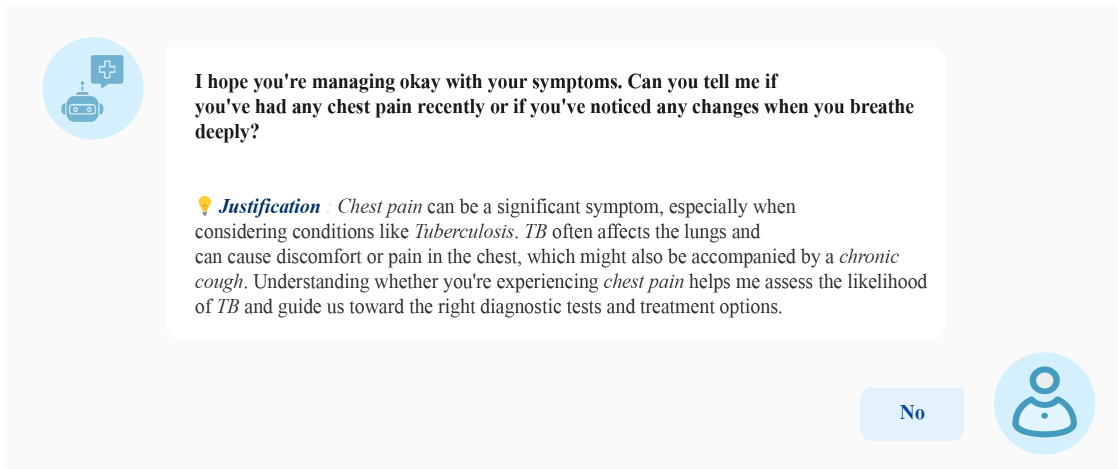


Figure 5: Justification for Symptom Question Selection

3.9.2 Real-Time Diagnostic State Updates

The system gives the accumulation of evidence in this by updating the diagnostic state, as the user responds 6. This involves confirmed and rejected symptoms and their scores of severity and the changes in likelihood of each potential disease. The presentation of the revised list of leading diseases allows the user to know how new data either substantiate or refute the diagnosis and make the process transparent and easy to follow.

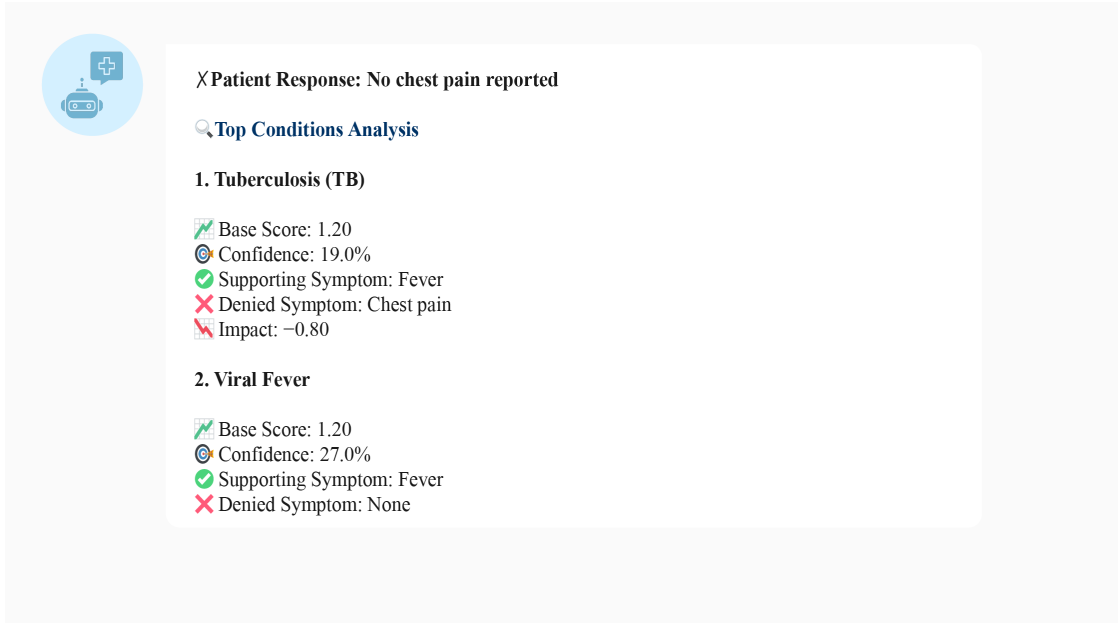


Figure 6: Real-Time Diagnostic State Updates

3.9.3 Test-Based Reasoning and Disease Elimination

At Phase Two, the system switches to the utilization of diagnostic techniques that narrow down the diagnosis 7. In the case of every disease the LLM explains the usefulness of every test and how the results will be used towards the diagnosis. Results of the tests are analyzed against preset levels and basing on the results, the diseases are either dismissed or accepted. This guarantees that the actions rely on explicit and rational rules, thus doing away with the ambiguity of the black-box reasoning.

Evaluating: Tuberculosis (TB)

💡 This test helps us look for the presence of acid-fast bacteria, which can indicate tuberculosis. It's an important step in diagnosing the condition.

Have you had a sputum smear test done recently? It's a simple lab test where they check a sample of your mucus from a cough to see if there are any signs of TB.

Yes. 3/100

Evaluating: Anemia

💡 The serum ferritin test measures the amount of ferritin in your blood, which is a protein that stores iron. Low levels can indicate anemia, so it's a helpful test to see how your iron levels are doing.

Have you had a serum ferritin test done recently? It's a simple blood test that helps us check the iron levels in your body, which is important for diagnosing anemia

Yes. 50 ng/mL

Figure 7: Test-Based Reasoning and Disease Elimination

3.9.4 Evidence-Linked Final Diagnosis and Referral

After the system makes the diagnostic shortlist stable, it provides a clear description of the most probable diagnosis, supported by the most important symptoms, test outcomes, and risk factors. 8. It then gives practical recommendations to the patient of what to do now, what to do later and what to look out of. Also, the system recommends the most

appropriate kind of medical expert to consult and the diagnosis becomes a complete course of action and follow-up channel.



Assessment (Based on symptoms and test results):

- 1. Most Likely Diagnosis with Confidence Level**
 - Diagnosis: Tuberculosis (TB)
 - Confidence Level: High
- 2. Explanation (Why this diagnosis fits best)**
 - Positive Sputum Smear Microscopy test indicates the presence of acid-fast bacilli, strongly confirming TB.
 - Symptoms such as fatigue, fever, decreased appetite, and headaches are consistent with TB.
 - Overlap with viral fever noted, but positive sputum result strongly favors TB.
 - Serum Ferritin test was negative, making anemia unlikely.
- 3. Relevant Risk Factors**
 - Close contact with TB patients
 - Weakened immune system (e.g., HIV, chronic illness)
 - Residence or travel in TB-prevalent areas

Figure 8: Evidence-Linked Final Diagnosis



Assessment (Based on symptoms and test results):

- 4. Recommended Next Steps**
 - Initiate standard 6-month TB treatment regimen (isoniazid, rifampin, pyrazinamide, ethambutol).
 - Ensure adequate caloric intake & balanced diet.
 - Regular follow-ups with healthcare provider for monitoring & adherence.
 - Additional tests: Chest X-ray, TB PCR for infection assessment.

Alternative Consideration: Viral Fever

Supporting evidence: fatigue, headache, body aches, fever, decreased appetite

Medical Disclaimer

This AI-generated assessment is for educational purposes only.
Always consult qualified healthcare professionals for:

- Formal medical diagnosis and treatment
- Interpretation of test results
- Clinical decision-making

Figure 9: Evidence-Linked Referral and Management

3.9.5 Rationale for the Step-by-Step Approach

The explainability design promises to transform a linear reasoning procedure that is transparent and clear enough to resemble an actual clinical consultation. All the decisions, including choice of symptoms to entering tests interpretation, are reasoned on each step building trust in the system. This will not only help establish trust in the decisions made by the chat bot, but also enable the validation of the reasoning to be tested and make every exercise consistent during diagnostic process.

3.9.6 Disease-Symptom Attribution Map

In order to increase the transparency of the diagnostic reasoning process carried out by our model, a per-disease–symptom attribution visualization is provided in our system for each patient-reported symptom, illustrating how it affects the scores of different diseases. Rather than generating a diagnosis within a black box, the system records which symptoms contribute most heavily to each disease. As the user responds with “yes” or “no” for symptoms during the conversation, the model continuously updates their respective weights for each of the diseases. Once a symptom is confirmed, the diseases that are frequently associated with that symptom are scored higher.

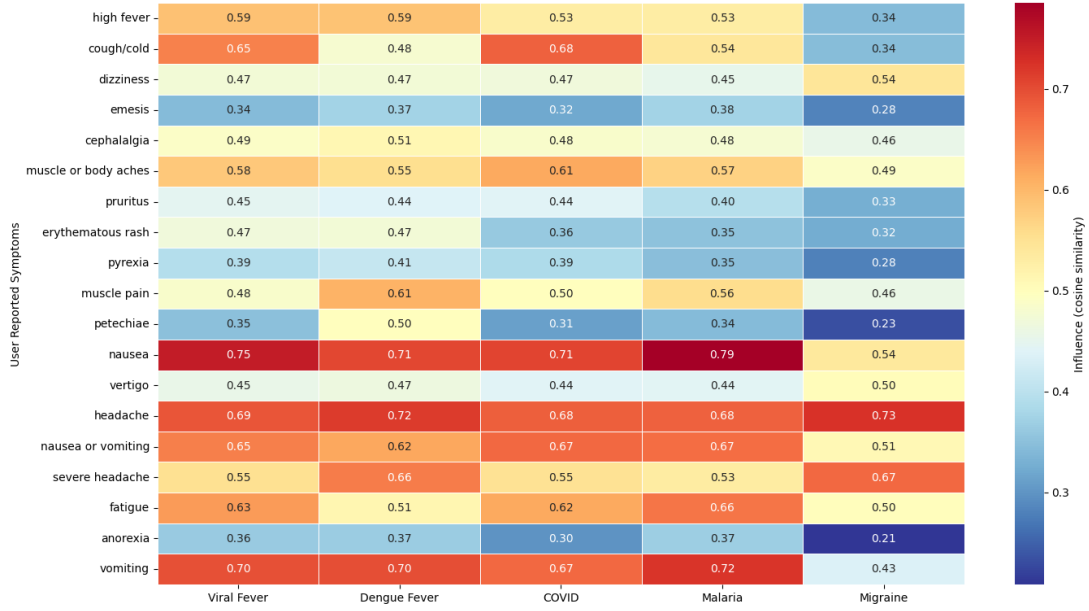


Figure 10: Disease–Symptom Attribution Heatmap generated by the system

Figure 10 presents the disease–symptom attribution heatmap created by the system. In this figure, the rows correspond to symptoms as reported by the patient, and the columns represent the candidate diseases considered for diagnosis. Each colored cell indicates how a symptom influences the likelihood of a specific disease. Dark red areas denote strong connections, indicating that the symptom played a crucial role in supporting that disease, while lighter shades and blue regions indicate weaker relationships. This variation demonstrates how the model distinguishes between highly informative and context-dependent features during diagnostic reasoning.

3.10 Machine Learning Models for Baseline Comparison

We also trained multiple base Machine Learning (ML) models that we could compare the performance of to the proposed LLM-based conversational disease diagnosis chatbot. By selecting these models, it was aimed to employ such popular methods of text classification and diagnosing in medicine. The models that were tested has been given:

1. Naive Bayes (NB): A simple yet efficient classifier that works well with high-dimensional text data.
2. Logistic Regression (LR): Used for binary and multi-class classification, assuming linear relationships.
3. Support Vector Machine (SVM): A margin-based classifier that works well with high-dimensional spaces.
4. Random Forest (RF): An ensemble method that builds multiple decision trees for more robust predictions.
5. k-Nearest Neighbors (KNN): A non-parametric method that classifies based on the majority of nearest neighbors.

To ensure a fair comparison, all models were trained on the same pre-processed dataset, using the same processing steps as the LLM knowledge base. Hyperparameters were optimized using cross-validation to ensure the best performance.

3.11 Evaluation Methods

We evaluated the conversational disease diagnosis chatbot using both traditional classification metrics and medical-specific assessments. These metrics not only check diagnostic accuracy but also the consistency of symptom interpretation, which is crucial in medical contexts.

3.11.1 Accuracy (ACC)

Accuracy measures the overall correctness of the model by comparing predicted labels to actual labels. It includes both correct positive and correct negative predictions.

$$\text{Accuracy} = \frac{TP + TN}{TP + TN + FP + FN} \quad (12)$$

Where:

TP (True Positives): Correctly predicted disease/symptom as present.

TN (True Negatives): Correctly predicted disease/symptom as absent.

FP (False Positives): Incorrectly predicted disease/symptom as present.

FN (False Negatives): Incorrectly predicted disease/symptom as absent.

3.11.2 Precision (PREC)

Precision measures how many of the positive predictions were actually correct. In medical diagnostics, high precision means fewer false positives.

$$\text{Precision} = \frac{TP}{TP + FP} \quad (13)$$

3.11.3 Recall (Sensitivity)

Recall measures how well the model identifies true positive cases, indicating the ability to recognize all relevant diseases or symptoms.

$$\text{Recall} = \frac{TP}{TP + FN} \quad (14)$$

3.11.4 F1-Score

F1-Score balances precision and recall, offering a balanced metric when both false positives and false negatives are critical.

$$\text{F1-score} = \frac{2 \times \text{Precision} \times \text{Recall}}{\text{Precision} + \text{Recall}} \quad (15)$$

These evaluation metrics provide a comprehensive view of the chatbot's performance, ensuring it is both accurate and reliable in interpreting symptoms.

4 Results and Discussion

4.1 Performance Evaluation of LLM System

Table 4 is a summary of the overall system performance of the LLM-based diagnostic system in all the test folds. The findings show that the model is highly diagnostic and has high general reliability. The system has the highest Accuracy of 90.3% which is Top-1 and the standard deviation is low ($\pm 9.5\%$), which indicates that the main predictions of the system are always correct on various subsets of evaluation. Top-3 Accuracy stands at 100% and this is in line with the fact that the correct diagnosis is never omitted among the top three conditions that the prediction model predicts.

Diagnostic system has Very Good Precision (85.8%), Recall (88.0%), and F1-Score (86.1%) with moderate fold-to-fold variation. Both the high recall and high precision values show that the system can identify most of the relevant conditions and reduce false positives respectively. The overall F1-Score indicates a balanced performance in terms of sensitivity and specificity. Altogether, Table 4 shows that the LLM system offers strong and clinically relevant diagnostic forecasts of different cases.

Figure 11 provides a comprehensive visualization of the LLM's performance across all key metrics, illustrating the balanced nature of the system's diagnostic capabilities.

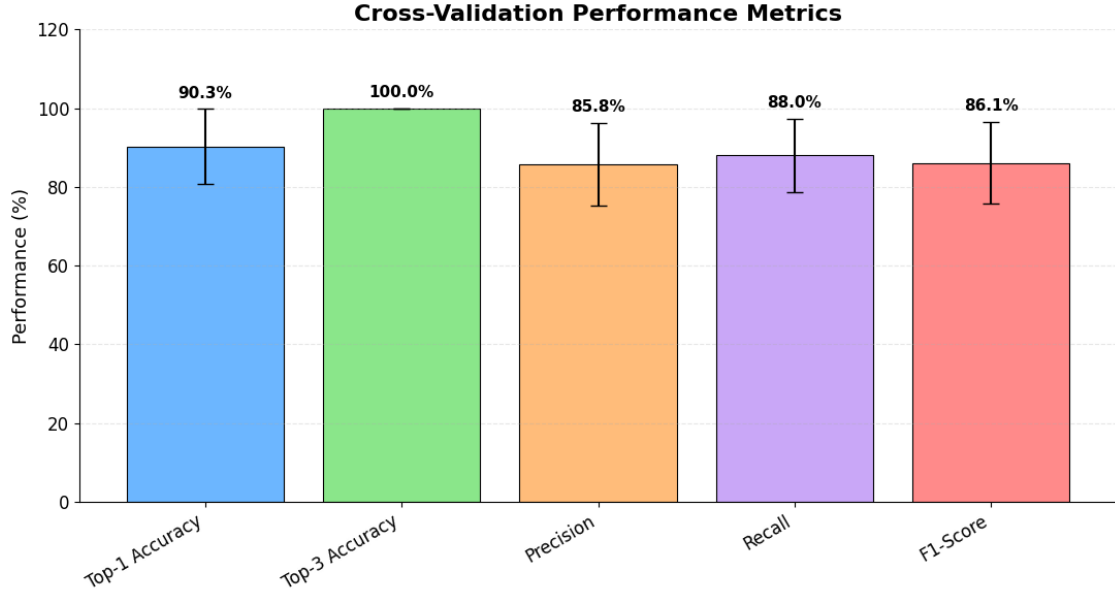


Figure 11: LLM Diagnostic System Performance Metrics

Table 4: Performance Overview of the LLM-Based Diagnostic System

Metric	Mean \pm Std. Dev.	Range	Interpretation
Top-1 Accuracy	90.3% \pm 9.5%	75.0% – 100.0%	Very High
Top-3 Accuracy	100.0% \pm 0.0%	100.0% – 100.0%	Very High
Precision	85.8% \pm 10.5%	70.8% – 100.0%	Very Good
Recall	88.0% \pm 9.4%	75.0% – 100.0%	Very Good
F1-Score	86.1% \pm 10.4%	72.2% – 100.0%	Very Good

4.2 Fold-wise and Stability Analysis

Table 5 shows fold-wise outcome of the 5-fold cross-validation experiment, which, in addition, says about the stability and generalizability of the diagnostic system. The model demonstrates high results throughout every fold though there is noticeable variation. Top-1 scores are between 75.0% and 100.0% which means that the system is very good in the majority of folds, but there are groups of patient instances where the system is more difficult to diagnose.

Even with these differences in the exact-match accuracy, Top-3 Accuracy is 100 percent in all folds, indicating that the model is highly effective, the correct diagnosis is available in the top three predictions no matter which test subset is used. Precision, recall, and F1-Score also show high interfold behavior, which indicates consistency in recognizing and ranking of correct diagnoses.

The confirmation of the fold-wise analysis is that the system has good diagnostic performance and strength under varying patient case distributions. The stability of the Top-3 Accuracy score and the close proximity of the precision/recall scores imply that the model is not especially vulnerable to a particular subset of the data, which should, in its turn, prove that this model can be used in the real world.

Table 5: Fold-wise Performance of the LLM-Based Diagnostic System

Fold	Cases	Top-1 Accuracy	Top-3 Accuracy	Precision	Recall	F1-Score
1	17	94.1%	100.0%	0.875	0.917	0.889
2	17	100.0%	100.0%	1.000	1.000	1.000
3	17	88.2%	100.0%	0.708	0.750	0.722
4	17	94.1%	100.0%	0.875	0.900	0.886
5	16	75.0%	100.0%	0.833	0.833	0.807

4.3 Disease-wise Performance Analysis

There was a wide variation in the performance of the system in terms of the various diseases available, which brought out significant insights into the diagnostic performance of the system. There were three groups of performance based on accuracy and confidence scores that we observed.

This analysis was done over 540 turns of evaluated conversation with the model while stating the symptoms in each turn. Table 6 provides disease-wise diagnostic accuracy of Top-1 and Top-3. Most of the conditions, including the Acute Diarrheal Illness, Dengue Fever, COVID-19, Irritable Bowel Syndrome, Migraine, Anxiety Disorders, Tuberculosis, Anemia, Depression, Asthma, and GERD, received 100% Top-1 accuracy, which shows that the system consistently selected the correct diagnosis as the most likely outcome of each case in those categories. The diagnostic patterns of these diseases are likely to have a combination of symptoms that are relatively unique in the dataset, which allows the separation in embedding space to be clear, and reduce confounding with other conditions. The similarity-based scoring algorithm of the model, therefore, can discriminate their clusters of symptoms with high reliability.

In comparison, Malaria, Hepatitis B, and Viral Fever did not obtain an ideal Top-1 accuracy despite all of them exhibiting 100% Top-3 accuracy. This trend implies that although the system will always admit them as relevant when making inferences, their ultimate order is at times overridden by other clauses. It is possible to explain the decreased Top-1 accuracy of these three diseases by the excessive overlap of the symptoms they have with a number of other diseases that are represented in the corpus. The traits of each of these conditions are broad and non-specific symptoms, which are seen in a wide range of diseases of infection and systemic diseases, and make the disease vectors less distinctive in the embedding space.

Moreover, these diseases often compete with conditions that include symptoms carrying higher semantic or clinical weight. In the scoring system of the system, symptoms with more diagnostic intensity or specificity have a more powerful effect on the ultimate ranking. In cases where competing diseases have semantically richer or more distinctively related symptom descriptors with their symptom pattern of disease, their score can outdo Malaria, Hepatitis B or Viral Fever, even when all are alike in their symptom patterns. This creates sensitivity in the end ranking to the minor differences in representational strength of associated symptoms which causes the actual disease to be sometimes moved off the top of the list.

In general, the disease specific outcomes are those of an expected behavior of a similarity-based diagnostic model acting in a field with a number of conditions that share generalized symptomatology. Although top-1 accuracy is lower with Malaria, Hepatitis B and Viral Fever because they have relatively non-discriminative symptom profiles, their top-3 accuracy proves that the system will invariably present them as plausible clinical diagnoses.

Table 6: Disease Performance Overview Sorted by Accuracy

Disease	Top-1 Accuracy (%)	Top-3 Accuracy (%)	Unique Symptoms
Acute Diarrheal Illness	100	100	loose stools, fever, loose motions
Dengue Fever	100	100	pain behind my eyes, joint pain, retro-orbital pain
COVID-19	100	100	loss of taste/smell, cough, shortness of breath
Irritable Bowel Syndrome (IBS)	100	100	distention, diarrhea, gas
Migraine	100	100	head pain, sensitivity to light, sensitivity to noise
Anxiety Disorders	100	100	irritability, can't sit still, fatigue
Tuberculosis (TB)	100	100	coughing up blood, dry cough, cough
Anemia	100	100	pale skin, cold hands and feet, difficulty breathing
Depression	100	100	thoughts of self-harm, feeling worthless, fatigue
Asthma	100	100	chest tightness, coughing a lot, tight feeling in chest
Gastroesophageal Reflux Disease (GERD)	100	100	chest pain, burning in chest, belching
Malaria	83.33	100	skin turning yellow, fever, chills
HepatitisB	50	100	skin turning yellow, exhaustion, fatigue
Viral Fever	33.33	100	head pain, aching head, fever

4.4 Comparative Analysis with Traditional ML Models

In order to put the performance of our LLM system into perspective, we made a thorough comparison with the conventional machine learning models. Five existing algorithms (Naive Bayes, Logistic Regression, SVM, Random Forest, and KNN) were tested on two feature extraction approaches (TF-IDF and CountVectorizer).

The conventional ML models were very diverse in terms of performance depending on the methods of feature extraction. TF-IDF was better than Count Vectorizer in all of the models. Naive Bayes performed the best using TF-IDF, with the F1-score of 0.864, then SVM (0.852), and Logistic Regression (0.820). Conversely, the two models that used CountVectorizer after that were infinitely worse with Naive Bayes decreasing to an F1-score of 0.616 and Logistic Regression to 0.159 (Figure 12).

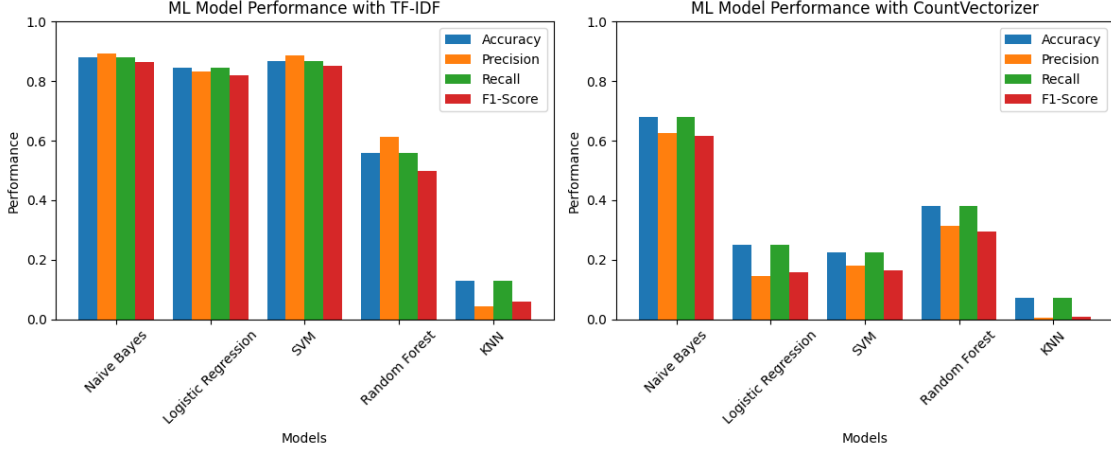


Figure 12: Performance Metrics of ML Models with TF-IDF and CountVectorizer Feature Extraction

The metrics of accuracy are a vivid demonstration of the general performance difference between the traditional models and the system based on the LLM. This is higher than Naive Bayes with TF-IDF (0.881) and much higher than its CountVectorizer equivalent (0.679) and the LLM has an accuracy of 0.903. Besides, the LLM has one more beneficial property in its ranked prediction, which can reach a perfect top-3 accuracy of 1.000, which the traditional models cannot offer as they only give a single class. The top-3 measure is especially crucial in clinical practice, where offering a variety of high-confidence alternative diagnoses can be used to support decision-making.

TF-IDF Naive Bayes is a little bit more precise with 0.893 as compared to 0.858 of the LLM with positive prediction being more specific. Once again, however, CountVectorizer version remains somewhat unreliable with a precision of 0.627 indicating sensitivity of these models to the option of feature extraction method. Values of recall indicate that the LLM (0.880) works nearly the same as the TF-IDF Naive Bayes baseline (0.881) and thus it has high capacity to preference true positives in both methods. CountVectorizer Naive Bayes model is significantly behind with the lowest recall of 0.679, which further supports its vulnerability to various measures.

Lastly, the F1-score that combines both precision and recall in a single measure shows the stability of the best performing models. TF-IDF Naive Bayes with a F1-score of 0.864 is then followed by the LLM with 0.861- this indicates that the LLM yields similar balances even though it has more reasoning ability. Contrarily, CountVectorizer model reduces drastically to 0.616. All in all, the accuracy and robustness as well as the diagnostic flexibility of the LLM are higher, and the TF-IDF Naive Bayes proves to be the most successful among the traditional baselines, whereas the CountVectorizer-based models have serious performance limits.

4.5 Ablation Study

4.5.1 Initial Ablation With All Parameters Enabled (All-MiniLM-L6-v2)

The first phase of the ablation study was conducted using the All-MiniLM-L6-v2 embedding model while keeping every system parameter turned on. These were minimum requirement of questions, minimum requirement of symptoms, level of confidence, maximum number of questions to be asked and similarity level. It was aimed at defining how sensitive the diagnostic system is to individual constraints and which parameters have a significant effect on predictive behaviour. The entire findings are presented in Table 7.

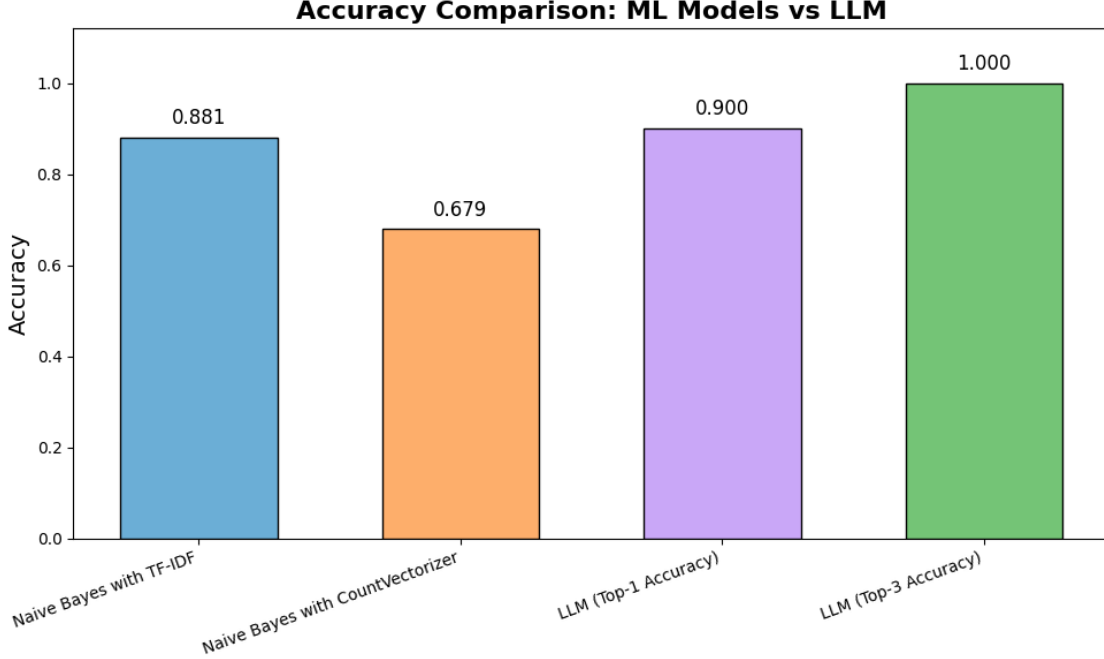


Figure 13: Accuracy Comparison of Best Performing ML Model (Naive Bayes with TF-IDF and CountVectorizer) vs. LLM

Table 7: Initial Ablation Results Using All-MiniLM-L6-v2 With All Parameters Enabled

Config	MinQ	MinS	Conf	MaxQ	Sim	Top1	Top3	Prec	Rec	F1	AvgQ	Lat.
Baseline	10	8	70.00	20	0.55	0.90	1.00	0.92	0.90	0.90	19.69	0.60
MinQ=5	5	8	70.00	20	0.55	0.90	1.00	0.92	0.90	0.90	19.69	3.13
MinQ=15	15	8	70.00	20	0.55	0.90	1.00	0.92	0.90	0.90	19.69	2.93
MaxQ=10	10	8	70.00	10	0.55	0.89	1.00	0.90	0.89	0.89	10.00	1.91
MaxQ=15	10	8	70.00	15	0.55	0.88	1.00	0.91	0.88	0.88	15.00	2.89
MinS=2	10	2	70.00	20	0.55	0.76	0.80	0.85	0.76	0.76	19.71	3.30
MinS=4	10	4	70.00	20	0.55	0.82	0.93	0.88	0.82	0.83	19.81	2.57
MinS=6	10	6	70.00	20	0.55	0.88	0.94	0.91	0.88	0.88	19.76	3.27
Conf=60	10	8	60.00	20	0.55	0.90	1.00	0.92	0.90	0.90	19.69	1.88
Conf=80	10	8	80.00	20	0.55	0.90	1.00	0.92	0.90	0.90	19.69	1.78
Sim=0.45	10	8	70.00	20	0.45	0.88	1.00	0.90	0.88	0.87	19.74	4.95
Sim=0.75	10	8	70.00	20	0.75	0.82	0.99	0.77	0.82	0.79	19.73	6.38
Sim=0.85	10	8	70.00	20	0.85	0.92	0.99	0.88	0.92	0.89	19.73	3.75

Baseline configuration shows excellent performance consisting of the Top-1 accuracy of 0.9048, a perfect Top-3 accuracy, and consistent precision, recall, and F1-score. The model in its nature poses close to twenty questions irrespective of limitations, which validate that the model tries to gather a rich enough symptom profile until a prediction is made. This base gives clear comparison of the changes in the parameters later.

Effect of Maximum Question Limit : Differences in the maximum number of questions give evident behaviour changes. In case the system is limited to ten questions, Top-1 accuracy reduces to 0.8929 because of poor symptom availability. A fifteen question cutoff results in a comparable drop. This denotes that high-confidence predictions require a large question budget. Although the question limit will help to cut down the length of conversation, it will compromise the quality of diagnosis.

Effect of Minimum Symptom Requirement : One of the most dominant parameters appears to be the minimum number of confirmed symptoms. The threshold reduction to two symptoms leads to a steep decrease in accuracy to 0.5952. The threshold set at four increases performance by a significant margin and the threshold set at six gives accuracy at 0.8809. These findings indicate that the model depends a lot on the depth of symptoms to make proper inferences. Notably, the stability of the performance occurs between six and eight confirmable symptoms implying that a MinS range of 6 to 8 has a high diagnostic reliability without excessive redundancy of questions.

Effect of Similarity Threshold : Modifying the similarity threshold has non-linear effects that are predictable. Such a low threshold (0.45) promotes excessively permissive matching, inflated false positives, and reduced F1 score. The increased threshold (0.75) is too restrictive and does not allow the genuine symptoms to match. It is interesting to note that 0.85 provides the highest accuracy of Top 1 (0.9167) at cost of greater latency. This confirms the fact that stricter matching is more precise but it involves more processing time.

Confidence Threshold and Minimum Questions : Two parameters did not demonstrate any detectable effect on diagnostic performance the minimum number of necessary questions and the confidence threshold. In all settings, alterations to these parameters brought the same Top 1 accuracy, precision, recall, and F1 score. This signifies that natural behaviour of the model already exceeds these limits thus they will not work effectively as regulatory restrictions.

The next stage of the ablation eliminated these parameters according to this evidence. The choice was based on purely scientific considerations: parameters that have no effect on the results should not be part of the decision pipeline of the system since they are not only hard to interpret but also are of no practical use.

4.5.2 Refined Ablation Without Confidence Threshold or Minimum Questions

Once the confidence threshold was set to 0 and the minimum number of questions had been passed, the ablation was again run with a simplified configuration space. The findings (Table 8) verify the previous ones. The limit of questions still has an influence on accuracy, especially when it is limited to ten or fifteen questions. The minimum symptom requirement once more exhibits the greatest effect, and the accuracy drops to its lowest point when MinS=2 is demanded and increases with further strengthened requirements to the agreed number of confirmed symptoms. The stabilisation of the performance at a MinS value of 6-8 again proves that this is the optimal operating range.

Table 8: Final Ablation After Removing Confidence Threshold and Minimum Question Requirement

Config	MinQ	MinS	Conf	MaxQ	Sim	Top1	Top3	Prec	Rec	F1	AvgQ	Lat.
Baseline	10	8	0.00	20	0.55	0.90	1.00	0.92	0.90	0.90	19.69	1.55
MaxQ=10	10	8	0.00	10	0.55	0.89	1.00	0.90	0.89	0.89	10.00	2.28
MaxQ=15	10	8	0.00	15	0.55	0.88	1.00	0.91	0.88	0.88	15.00	2.42
MinS=2	10	2	0.00	20	0.55	0.60	0.80	0.66	0.60	0.58	11.75	2.26
MinS=4	10	4	0.00	20	0.55	0.82	0.90	0.87	0.82	0.83	14.63	2.30
MinS=6	10	6	0.00	20	0.55	0.88	0.94	0.91	0.88	0.88	18.25	2.37
Sim=0.45	10	8	0.00	20	0.45	0.88	1.00	0.90	0.88	0.87	19.74	2.78
Sim=0.75	10	8	0.00	20	0.75	0.82	0.99	0.77	0.82	0.79	19.73	3.21
Sim=0.85	10	8	0.00	20	0.85	0.92	0.99	0.88	0.92	0.89	19.73	4.01

The similarity threshold acts like the previous observations: the lower the threshold, the worse the accuracy, the moderate thresholds yield acceptable accuracy, and the higher the precision, the higher the latency. Since the confidence level and required minimum number of questions did not have any impact in both stages of ablation, this latter table shall be regarded as the last ablation table which has been validated under the All-MiniLM-L6-v2 model.

4.5.3 Embedding Model Comparison: All-MiniLM-L6-v2 vs. Text-Embedding-Ada-002

The ablation was once again repeated to test the potential of the text-embedding-ada-002 model to provide better diagnostic performance. Even though ada-002 shows moderate performance, the results reveal evident drawbacks compared to All-MiniLM-L6-v2. There are generally reduced accuracy levels when used in more than two configurations and the model is more sensitive to changes in minimum symptoms or maximum questions, which means less stability. The table can be found at Table 9

Table 9: Ablation Results Using Text-Embedding-Ada-002

Config	MinQ	MinS	Conf	MaxQ	Sim	Top1	Top3	Prec	Rec	F1	AvgQ	Lat.
Baseline	10	8	0.00	20	0.55	0.92	0.99	0.88	0.92	0.89	19.79	3.49
MaxQ=10	10	8	0.00	10	0.55	0.87	0.98	0.89	0.87	0.85	10.00	1.87
MaxQ=15	10	8	0.00	15	0.55	0.88	0.99	0.84	0.88	0.86	15.00	3.04
MinS=2	10	2	0.00	20	0.55	0.63	0.74	0.72	0.63	0.62	11.39	1.86
MinS=4	10	4	0.00	20	0.55	0.77	0.87	0.82	0.77	0.78	13.57	3.13
MinS=6	10	6	0.00	20	0.55	0.90	0.96	0.93	0.90	0.90	18.23	3.38
Sim=0.45	10	8	0.00	20	0.45	0.92	0.99	0.88	0.92	0.89	19.79	3.65
Sim=0.75	10	8	0.00	20	0.75	0.92	0.99	0.88	0.92	0.89	19.79	4.21
Sim=0.85	10	8	0.00	20	0.85	0.89	0.98	0.91	0.89	0.88	19.75	3.77

The major disadvantage with ada-002 is that it has a much higher latency. Although the same can be seen in the average values of the recorded latency, the effect was even greater in case of live diagnostic testing, where the ada-002 actually produced slower answers. It reduces the usability and interrupts the flow of conversation, which is not appropriate in interactive diagnosis based on the symptoms. It is based on these reasons that All-MiniLM-L6-v2 was chosen as the embedding model to be used by the final system.

4.5.4 Scoring Weight Ablation

The last ablation (Table 10) aims at considering the various weighting techniques in taking global and local similarity scores into the diagnostic system. Global similarity scoring compares the similarity of symptoms that the user confirms compared to the general symptom profile of each disease in its entirety. By contrast, local similarity scoring scores matches of the symptoms at the symptom level with a preference made on fine-grained, direct correspondence between what is typed by the user and the symptoms of a particular disease. Global scoring is a general signal of structural similarity and local scoring offers specific symptom accuracy. The question in this ablation was to find an optimum between these two points of view.

Table 10: Scoring Weight Ablation: Global vs. Local vs. Hybrid Similarity

Config	G_w	L_w	Top1	Top3	Prec	Rec	F1
Local_Only	0.00	1.00	0.89	0.98	0.91	0.89	0.89
Global_Only	1.00	0.00	0.74	0.98	0.79	0.74	0.72
Hybrid_70_30	0.70	0.30	0.90	1.00	0.92	0.90	0.90
Hybrid_50_50	0.50	0.50	0.90	0.99	0.92	0.90	0.90

The evidence shows that there are apparent distinctions in scoring strategies. The worst scoring system is a purely global scoring system, with the highest accuracy of Top-1 at 0.7381, meaning that the similarity between diseases is not enough to be accurately diagnosed. Local-only scoring is significantly more effective (Top-1 accuracy of 0.8929), whereas fine-grained symptom matching is much more diagnostic than global disease similarity. Nevertheless, local-only scoring is yet to provide the more comprehensive contextual cue that is useful in differentiating clinically similar diseases.

The limitations are solved by hybrid scoring that combines both local and global similarity. The 70/30 hybrid (global/local) and the 50/50 hybrid both obtained high and stable scores, and the Top-1 accuracy scores are 0.9048 and the performance is as good or better than the baseline. These hybrids take on the fine specificity of local scoring, and general contextual frame offered by global scoring. Consequently, hybrid weighting delivers the most trustworthy diagnostic behaviour and it was decided to be the final scoring strategy of the system.

4.6 Bias Mitigation and Hallucination Control

4.6.1 Bias Mitigation

The medical large language models can be biased in the form of focusing on specific diseases too much, misinterpreting the words used by the user or lack of evidence to draw a conclusion. In order to mitigate such effects, various multi-layered mitigation measures were used in this system. The model was first founded on a retrieval-augmented generation (RAG) framework, which helps to retrieve confirmed information in authoritative medical PDFs before each reasoning step. This makes sure that the responses and symptom extraction of the model is founded on factual and evidence-based sources as opposed to probable associations gained in the course of pretraining.

Second, a validation layer of PDF format was introduced to check all the symptoms or diagnostic questions generated by the LLM against the structured knowledge retrieved at the uploaded guideline documents. This approach eliminates spurious associations and limits the model reasoning to medically established things.

Third, user inputs were standardized using linguistic normalization and synonym mapping (e.g., “tiredness” became “fatigue,” “blood in urine” became “hematuria”), avoiding interpretative bias due to differences in natural language expression. A weighted confidence scoring system was also introduced to scale the severity and relevance of the symptoms to avoid the system overestimating common symptoms, but with no clinical importance. Penalties on negative symptoms, which occur when the user disbelieves a symptom, also provide further balance of inference, giving attention to positive and negative evidence.

Lastly, nonlinear scaling and capped confidence (maximum 95%) avoids overconfidence making predictions and helps to be aware of uncertainty, without which responsible AI-assisted diagnosis cannot exist. All these mechanisms contribute to the minimization of linguistic and diagnostic bias, which makes the process of decision-making by the system proportionate, transparent, and medically based.

4.6.2 Hallucination Control

Large language models are more susceptible to hallucinations and this is particularly dangerous in the medical field where they can create non-existent symptoms, tests, or diagnoses. The suggested system involves a multi-level hallucination control pipeline that involves retrieval grounding, semantic validation and confidence control.

We have used Grounded Generation method which makes sure that all outputs of the LLM are based on medically validated textual context retrieved in the PDF-based knowledge base, both the symptom extraction and the question generation. Besides grounding, there can be a clear mechanism of validation that would validate any LLM-generated symptom or follow-up question. The generated symptoms that are not present in the validated database are eliminated before they are incorporated in the diagnostic process of reasoning.

The language outputs are further whittled down to the clinically relevant entities by a two-stage normalization chain which consists of symptom extraction and standardization of medical terms. Within the embedding space, threshold-based cosine similarity filtering (conservative cutoff of 0.55) and synonym-aware matching limit symptom recognition to semantically consistent pairs, reducing false associations and overgeneralization.

Last but not least, the moderation mechanisms (confidence scaling, multi-factor computation of confidence and multi-phase confirmation (inference by the symptoms and verification by the diagnostic test) are such that the model does not rest on false conclusions too soon. This pseudo reasoning, along with active rejection of outputs that are unprovable, is an effective way of minimizing hallucinations and brings system outputs into line with known medical facts.

4.7 Clinical Applicability and Limitations

The clinical usefulness of this diagnostic model based on the LLM is that it can interpret symptoms in a way that is more or less similar to the reasoning of a human clinician and at the same time goes beyond conventional methods. In contrast to traditional machine learning systems which must assume fixed representations of features, the LLM is able to handle free-text descriptions of the symptoms, learn subtle linguistic information, and generate ranked differential diagnoses, which resembles the way clinicians consider multiple possibilities before making the final decision, as opposed to the traditional approach of focusing on a single possibility at once. Its optimal top-3 accuracy means that although the top-1 prediction is not accurate, the true diagnosis is an exceptionally likely one to be among the top-3 choices to assist in making a safe and accurate decision. In addition to this, the model exhibits more rigorous diagnostics because of the two-step reasoning process: once it has made predictions based on the symptoms, it carries out a second, more conclusive step based on the outcomes of laboratory tests. Through the interpretation of pertinent lab parameters and comparing them to disease-specific patterns, the system will be able to confirm or exclude conditions with greater confidence, which is representative of actual clinical practices where symptom assessment is accompanied by diagnostic testing. Such a sensitive core, solid capacity to process ambiguous patient information and the capability to complete a diagnosis based on the test data make the LLM an effective and efficient method of clinical decision support, triage routes, and remote consultation system.

Nevertheless, there are also a few limitations that must be mentioned. The quality of the medical knowledge base and the accuracy of the input of the user are also inherently related to the reliability of the system. These sources may have gaps or outdated information, or be missing any contextual detail which may directly influence the accuracy of the reasoning in the model and the consistency of the diagnosis. The test data used for the evaluations were synthetic dialogues which lacks real life patient interactions. Additionally, the system relied heavily on fixed assigned weights across various symptoms which made it inadequate to capture the symptom severity and relevance across different diseases. As a result, the system generated follow-up questions from predefined symptom sets rather than adapting its reasoning to individual clinical contexts.

These weaknesses indicate the areas of future investigation and enhancement of the system. The addition of more detailed information regarding problematic situations and an increase in the scope of capabilities of the system that might deal with vague data may further aid in the clinical application of the system.

5 Conclusion and Future Work

We have introduced a real-time explainable conversational Artificial Intelligence system that diagnoses early stage of the disease using Large Language Models. Our model, combines GPT-4o, Retrieval-Augmented Generation and Chain-of-Thought prompting to facilitate interpretable and interactive diagnostic dialogue. Evaluation against traditional machine learning models demonstrates superior performance in handling complex, conversational diagnostic scenarios, achieving 100% Top-3 accuracy and 88% recall.

The implications of such developments extend into the access to healthcare provision particularly in low-resource settings where access to experts is limited. The possibilities of the system in providing the health care delivery gap are that it provides accurate and approachable diagnostics direction by means of natural communication.

Future research directions include:

1. **Reinforcement Learning** : Making the model adaptable to different patient and disease context to handle unpredictable scenarios and learn over time from feedback.
2. **Multilingual Support:** The translation of the system into more languages to make it accessible in the areas of global delivery of healthcare.
3. **EHR Integration:** Linking to electronic health records (EHR) in order to include patient history and background.

As the AI system continues to evolve in the healthcare sector, there would be a need to ensure a balance between performance, transparency, and usability. Our work shows that such balance is possible with LLM-based systems, promising opportunities of more accessible, explainable and effective diagnostic assistance.

Declaration of Generative AI and AI-Assisted Technologies

During the preparation of this manuscript, the author(s) used *ChatGPT* to generate synthetic patient cases. Following the use of this tool, the author(s) reviewed and edited the content as necessary and take full responsibility for the accuracy, integrity, and originality of the published work.

Data and Code Availability

This study did not use any publicly available datasets. The knowledge base was constructed by curating information from authoritative publicly accessible sources, including guidelines and reports published by the World Health Organization (WHO) and other established medical organizations, all of which are cited in the manuscript. The source code for the proposed system, including the web-based implementation, model execution, and evaluation scripts, is available from the corresponding author upon reasonable request.

References

M.D. Abràmoff, P.T. Lavin, M. Birch, and et al. Pivotal trial of an autonomous ai-based diagnostic system for detection of diabetic retinopathy in primary care offices. *NPJ Digital Medicine*, 1:39, 2018. doi: 10.1038/s41746-018-0040-6.

G. Campanella, M.G. Hanna, L. Geneslaw, and et al. Clinical-grade computational pathology using weakly supervised deep learning on whole slide images. *Nature Medicine*, 25:1301–1309, 2019. doi: 10.1038/s41591-019-0508-1.

Centers for Disease Control and Prevention. Hepatitis b: Signs and symptoms, 2024a. URL <https://www.cdc.gov/hepatitis-b/signs-symptoms/index.html>. Accessed: 2025-12-19.

Centers for Disease Control and Prevention. Post-travel evaluation of the ill traveler, 2024b. URL <https://www.cdc.gov/yellow-book/hcp/post-travel-evaluation/post-travel-evaluation-of-the-ill-traveler.html>. Accessed: 2025-12-19.

Harrison Chase. LangChain: Building applications with LLMs through composability, 2023. URL <https://python.langchain.com/>. Accessed at 2025-08-01.

J. De Fauw, J.R. Ledsam, B. Romera-Paredes, and et al. Clinically applicable deep learning for diagnosis and referral in retinal disease. *Nature Medicine*, 24:1342–1350, 2018. doi: 10.1038/s41591-018-0107-6.

B. Ehteshami Bejnordi, M. Veta, P. Johannes van Diest, and et al. Diagnostic assessment of deep learning algorithms for detection of lymph node metastases in women with breast cancer. *JAMA*, 318:2199–2210, 2017. doi: 10.1001/jama.2017.14585.

A. Esteva, B. Kuprel, R.A. Novoa, and et al. Dermatologist-level classification of skin cancer with deep neural networks. *Nature*, 542:115–118, 2017. doi: 10.1038/nature21056.

Facebook AI. FAISS: A library for efficient similarity search, 2023. URL <https://github.com/facebookresearch/faiss>. Accessed at 2025-07-15.

A. C. Ford, A. D. Sperber, and et al. Global prevalence of and risk factors for irritable bowel syndrome: a meta-analysis. *The Lancet Gastroenterology & Hepatology*, 5(10):908–917, 2020. doi: 10.1016/S2468-1253(20)30217-X.

GBD 2021 Anaemia Collaborators. Global, regional, and national burden of anaemia, 1990–2021: a systematic analysis. *The Lancet Haematology*, 10:e737–e753, 2023. doi: 10.1016/S2352-3026(23)00140-7.

GBD 2021 Gastrointestinal Disorders Collaborators. Global burden of gastro-oesophageal reflux disease, 1990–2021: a systematic analysis. *Frontiers in Public Health*, 10:100105, 2022. doi: 10.3389/fpubh.2022.100105.

GBD 2021 Headache Collaborators. Global, regional, and national burden of migraine and headache disorders, 1990–2021: a systematic analysis. *The Lancet Neurology*, 22:881–896, 2023. doi: 10.1016/S1474-4422(23)00123-4.

V. Gulshan, L. Peng, M. Coram, and et al. Development and validation of a deep learning algorithm for detection of diabetic retinopathy in retinal fundus photographs. *JAMA*, 316:2402–2410, 2016. doi: 10.1001/jama.2016.17216.

G. K. Gupta, A. Singh, S. V. Manikandan, and A. Ehtesham. Digital diagnostics: The potential of large language models in recognizing symptoms of common illnesses. *AI*, 6(1):13, 2025. doi: 10.3390/ai6010013. URL <https://doi.org/10.3390/ai6010013>.

International Headache Society. Migraine – ichd-3, 2018a. URL <https://ichd-3.org/1-migraine/>. Accessed: 2025-12-19.

International Headache Society. Ichd-3 pocket version, 2018b. URL <https://ihs-headache.org/wp-content/uploads/2020/05/ICHD-3-Pocket-version.pdf>. Accessed: 2025-12-19.

Yoon Kim et al. Mdagents: An adaptive collaboration of llms for medical decision-making. NeurIPS 2024, 2024. URL <https://arxiv.org/abs/2404.15155>.

LangChain. Prompt templates documentation, 2023a. URL https://python.langchain.com/docs/modules/model_io/prompts/. Accessed at 2025-08-03.

LangChain. Text splitters documentation, 2023b. URL https://python.langchain.com/docs/modules/data_connection/document_transformers/. Accessed at 2025-08-07.

Matplotlib. Matplotlib documentation, 2023. URL <https://matplotlib.org/stable/contents.html>. Accessed at 2025-08-01.

Mayo Clinic. Viral gastroenteritis: Symptoms and causes, 2024. URL <https://www.mayoclinic.org/diseases-conditions/viral-gastroenteritis/symptoms-causes/syc-20378847>. Accessed: 2025-12-19.

Microsoft Azure. Azure OpenAI Embeddings Documentation, 2023a. URL <https://learn.microsoft.com/en-us/azure/ai-services/openai/how-to/embeddings>. Accessed at 2025-07-20.

Microsoft Azure. Azure OpenAI Service Documentation, 2023b. URL <https://learn.microsoft.com/en-us/azure/ai-services/openai/>. Accessed at 2025-07-12.

National Center for Biotechnology Information. Gastroesophageal reflux disease, 2023a. URL <https://www.ncbi.nlm.nih.gov/books/NBK554462/>. Accessed: 2025-12-19.

National Center for Biotechnology Information. Irritable bowel syndrome, 2023b. URL <https://www.ncbi.nlm.nih.gov/books/NBK534810/>. Accessed: 2025-12-19.

NumPy. Numpy documentation, 2023. URL <https://numpy.org/doc/stable/>. Accessed at 2025-07-30.

A. Omar, J. Smith, and et al. Deep learning applications in spondyloarthropathy imaging: a systematic review. *European Radiology*, 34:11261–11275, 2024. doi: 10.1007/s00330-024-11261-x.

Pandas. Pandas documentation, 2023. URL <https://pandas.pydata.org/docs/>. Accessed at 2025-07-28.

Phaseit. PyPDF2 documentation, 2023. URL <https://pythonhosted.org/PyPDF2/>. Accessed at 2025-07-22.

R. Poplin, A.V. Varadarajan, K. Blumer, and et al. Prediction of cardiovascular risk factors from retinal fundus photographs via deep learning. *Nature Biomedical Engineering*, 2:158–164, 2018. doi: 10.1038/s41551-018-0195-0.

P. Rajpurkar, J. Irvin, K. Zhu, and et al. Chexnet: Radiologist-level pneumonia detection on chest x-rays with deep learning. *arXiv preprint arXiv:1711.05225*, 2018.

Rome Foundation. Rome iv diagnostic criteria for irritable bowel syndrome, 2016. URL <https://theromefoundation.org/rome-iv/rome-iv-criteria/>. Accessed: 2025-12-19.

Scikit-learn. Model evaluation documentation, 2023. URL https://scikit-learn.org/stable/modules/model_evaluation.html. Accessed at 2025-07-25.

K. Singhal, S. Azizi, T. Tu, S. S. Mahdavi, J. Wei, H. W. Chung, N. Scales, A. Tanwani, H. Cole-Lewis, S. Pfohl, P. Payne, M. Seneviratne, P. Gamble, C. Kelly, N. Scharli, A. Chowdhery, P. Mansfield, B. Aguera y Arcas, D. Webster, G. S. Corrado, Y. Matias, K. Chou, J. Gottweis, N. Tomasev, Y. Liu, A. Rajkomar, J. Barral, C. Semturs, A. Karthikesalingam, and V. Natarajan. Large language models encode clinical knowledge. *arXiv preprint*, 2022. URL <https://arxiv.org/abs/2212.13138>.

H. Song, S. Kim, and et al. Deep learning–assisted diagnosis of acute mesenteric ischemia using ct angiography and clinical data. *Frontiers in Medicine*, 12:1510357, 2025. doi: 10.3389/fmed.2025.1510357.

Augustin Toma, Patrick R. Lawler, Jimmy Ba, et al. Clinical camel: An open expert-level medical language model with dialogue-based knowledge encoding. arXiv preprint, 2023. URL <https://arxiv.org/abs/2305.12031>.

E. Topol. *Deep Medicine: How Artificial Intelligence Can Make Healthcare Human Again*. Basic Books, 2019.

T. Tu, A. Palepu, M. Schaekermann, K. Saab, J. Freyberg, R. Tanno, A. Wang, B. Li, M. Amin, N. Tomasev, S. S. Mahdavi, C. Semturs, J. Gottweis, J. Barral, K. Chou, G. S. Corrado, Y. Matias, A. Karthikesalingam, and V. Natarajan. Towards conversational diagnostic AI. *arXiv preprint*, 2024. URL <https://arxiv.org/abs/2401.05654>.

R. Vazquez, Y. Liu, and et al. Machine learning and deep learning methods for cervical cancer: a comprehensive review. *Diagnostics*, 15(12):1543, 2025. doi: 10.3390/diagnostics15121543.

World Gastroenterology Organisation. Common gastrointestinal symptoms: Gerd, 2021. URL <https://www.worldgastroenterology.org/guidelines/common-gi-symptoms/common-gi-symptoms-english>. Accessed: 2025-12-19.

World Health Organization. Guidelines for the prevention, care and treatment of hepatitis b, 2015. URL <https://www.who.int/publications/i/item/9789240090903>. Accessed: 2025-12-19.

World Health Organization. Mental disorders fact sheet – anxiety disorders, 2019a. URL <https://www.who.int/news-room/fact-sheets/detail/mental-disorders>. Accessed: 2025-10-03.

World Health Organization. Asthma fact sheet, 2019b. URL <https://www.who.int/news-room/fact-sheets/detail/asthma>. Accessed: 2025-10-03.

World Health Organization. Depression fact sheet, 2019c. URL <https://www.who.int/news-room/fact-sheets/detail/depression>. Accessed: 2025-10-03.

World Health Organization. Diarrhoeal disease fact sheet, 2020. URL <https://www.who.int/news-room/fact-sheets/detail/diarrhoeal-disease>. Accessed: 2025-10-03.

World Health Organization. Hepatitis b fact sheet, 2023a. URL <https://www.who.int/news-room/fact-sheets/detail/hepatitis-b>. Accessed: 2025-10-03.

World Health Organization. Depression, 2023b. URL <https://www.who.int/health-topics/depression>. Accessed: 2025-12-19.

World Health Organization. Who guidelines for malaria, 2023c. URL <https://iris.who.int/bitstream/handle/10665/382254/B09514-eng.pdf>. Accessed: 2025-12-19.

World Health Organization. Who coronavirus (covid-19) dashboard – 2024 update, 2024a. URL <https://covid19.who.int/>. Accessed: 2025-10-03.

World Health Organization. Dengue situation update – april 2024, 2024b. URL <https://www.who.int/news-room/fact-sheets/detail/dengue-and-severe-dengue>. Accessed: 2025-10-03.

World Health Organization. World malaria report 2024, 2024c. URL <https://www.who.int/teams/global-malaria-programme/reports/world-malaria-report-2024>. Accessed: 2025-10-03.

World Health Organization. Global tuberculosis report 2024, 2024d. URL <https://www.who.int/publications/i/item/9789240094290>. Accessed: 2025-10-03.

World Health Organization. Anaemia fact sheet, 2024e. URL <https://www.who.int/news-room/fact-sheets/detail/anaemia>. Accessed: 2025-12-19.

World Health Organization. Coronavirus disease (covid-19) fact sheet, 2024f. URL [https://www.who.int/news-room/fact-sheets/detail/coronavirus-disease-\(covid-19\)](https://www.who.int/news-room/fact-sheets/detail/coronavirus-disease-(covid-19)). Accessed: 2025-12-19.

World Health Organization. Malaria fact sheet, 2024g. URL <https://www.who.int/news-room/fact-sheets/detail/malaria>. Accessed: 2025-12-19.

World Health Organization. Malaria: Questions and answers, 2024h. URL <https://www.who.int/news-room/questions-and-answers/item/malaria>. Accessed: 2025-12-19.

World Health Organization. Malaria, 2024i. URL <https://www.who.int/health-topics/malaria>. Accessed: 2025-12-19.

World Health Organization. Tuberculosis, 2024j. URL <https://www.who.int/health-topics/tuberculosis>. Accessed: 2025-12-19.